

Entanglement of a qubit with a single oscillator mode

Gregory Levine

Department of Physics and Astronomy, Hofstra University, Hempstead, NY 11549

V. N. Muthukumar

Department of Physics, Princeton University, Princeton, NJ 08544

(Dated: May 21, 2019)

We solve a model of a qubit coupled to a massive environmental oscillator mode where the qubit backaction is treated exactly. It is shown that the oscillator displacement only becomes effectively entangled with the qubit beyond a certain critical coupling and is decoupled at smaller coupling. We derive an effective action for the critical point in which the entangled state is defined by an instanton in the collective qubit-environment degree of freedom. The resulting model is shown to be formally equivalent to a Fluctuating Gap Model (FGM) of a disordered Peierls chain. Below the transition, a fraction of the qubit is entangled and a fraction remains coherent, but effectively damped with a lifetime proportional to an adiabatic parameter.

PACS numbers: PACS numbers: 03.65.Yz, 71.27.+a

The subject of quantum computing has led to renewed interest in the theory of quantum decoherence and also exposed a practical side to the theory. Scalable, persistent current designs for qubits involve measurement devices that are permanently coupled, leading to a continuous dephasing of the qubit^{1,2}. Before a quantum measurement can be made, the qubit must become entangled with the measurement device. The competing demands of quantum measurement and minimal dephasing is an active topic of study within the theory of mesoscopic quantum detectors^{3,4,5,6}.

In this letter, we study the problem of how a qubit becomes entangled with a single environmental mode when the qubit backaction on the environment is not neglected. This is perhaps the simplest quantum environment, but already displays great complexity. Models of dissipative quantum environments such as the spin-boson model (SBM) are intentionally weakly coupled and therefore neglect backaction. However, environments imposed by quantum detectors may be strongly coupled and exhibit sharp spectral features. Our results may be applied to any environment (e.g. detector or qubit-qubit coupler) that exhibits a low energy monochromatic spectrum; as an example, we discuss the environment imposed by an underdamped DC-SQUID detector. Lastly, we point out the equivalence between the present model and a particular model of disordered fermions.

Consider a qubit coupled to a single harmonic oscillator described by the Hamiltonian

$$H = \frac{1}{2m!} (a + a^\dagger)^2 + \frac{1}{2} \langle a^\dagger a \rangle \quad (1)$$

If the oscillator is replaced by a classical, adiabatic oscillator (the limit $m! \rightarrow 0, m!^2 \rightarrow \infty$), it is known that (1) exhibits a bifurcation at $\omega^2 = m!^2$ in that the energy of the ground state is now minimized by assuming a nonzero value of the oscillator displacement, $x = x_0$. In the doubly degenerate ground state, the qubit is localized with a nonzero expectation value, $\langle h_z \rangle \neq 0$. This

is the classical counterpart of quantum entanglement between the qubit and a displacement coherent state of the oscillator. The classical calculation begs two questions: 1) If the oscillator localizes the qubit, is all coherent behavior destroyed? 2) If the qubit and oscillator weakly interact ($\omega^2 \ll m!^2$) aren't they always entangled to some degree?

We show that the onset of entanglement with the oscillator displacement becomes discontinuous in the massive limit, with a particular projection of the qubit wavefunction playing the role of an order parameter in a second order phase transition. The fraction of the qubit that remains coherent becomes strongly damped below the transition. In terms of the qubit spectral function, spectral weight is transferred at the transition from the coherent feature at $\omega = 0$ to an exponentially small energy scale corresponding to the entanglement.

Entanglement of the qubit in our case is distinct from that of weak-coupling theories (such as the SBM) in that the ergodicity of the environment is effectively broken and fluctuations become non-Gaussian. This latter effect, of course, cannot be seen by integrating out the environmental degrees of freedom to find the effective action of the qubit. In this respect, our calculation bears some relation to the description of quantum measurement by Single Electron Transistor (SET) and overdamped DC-SQUID detectors^{3,4}. In this scheme, the qubit degrees of freedom are integrated out to yield the response function of the detector. However, the SET and overdamped DC-SQUID detectors are strongly dissipative devices; our calculation is relevant to a strongly underdamped detector such as the C-shunted DC-SQUID of ref¹.

To represent the qubit, we choose the finite temperature formalism of Popov and Fedotov⁷ in which the action is written in terms of spinors satisfying modified boundary conditions. The imaginary time action corresponding to (1) is

$$S = \int d\tau (\partial_\tau + \langle h_z \rangle) \partial_\tau + S_0 \quad (2)$$

where $S_0 = \frac{R}{d} \frac{1}{2m} \underline{x}^2(\) + \frac{1}{2} kx^2(\)$, $k = m!^2$ and $(\)$ is a spinor

$$(\) = \begin{pmatrix} w(\) \\ \#(\) \end{pmatrix}$$

The spin-1/2 is formally represented as a fermion spinor with an imaginary chemical potential. The latter eliminates unphysical fermionic states from the Hilbert space. A gauge transformation removes the chemical potential and shifts the Matsubara frequencies to $\omega_n = 2(n+1/4)$. Conventional finite temperature field theory techniques may now be applied to the action (2).⁷

Introducing the modified Fourier transform $s(\) = \int_{-\infty}^{\infty} (\omega_n) e^{i\omega_n t}$ the fermions may be integrated out to yield an effective boson action:

$$Z = \int_0^{\infty} D\omega_n D\omega_m \frac{e^{S_{\text{eff}}}}{D\omega_n D\omega_m e^{S_{\text{eff}}}}$$

$$S_{\text{eff}} = \text{tr} \log (G_0^{-1} + p = x(\omega_n - \omega_m)_z) + S_0$$

where $G_0 = (i\omega_n - x)^{-1}$ is the free fermion Green's function.

Expanding the action to quartic order in ϵ and regrouping into dynamical and static terms, respectively, we obtain:

$$\begin{aligned} S_{\text{eff}} &= \frac{1}{2} \int_0^{\infty} \left[(m p_n^2 + (p_n - 0) \dot{x}(p_n))^2 \right. \\ &+ \frac{1}{2} \int_0^{\infty} \left[(k + (0) \dot{x}(p_n))^2 \right. \\ &+ \left. \left. D(0) \dot{x}(p_n)^4 \right] \right] \end{aligned}$$

where the coefficients are given by

$$\begin{aligned} (p_n) &= -\text{tr} \frac{2}{\omega_n} G_0 (\omega_n - \omega_m)_z G_0 (\omega_m)_z \\ &= -\tanh \frac{4}{p_n^2 + 4} \\ D(0) &= \frac{4}{2} \text{tr} [G_0 (\omega_m)_z]^4 = \frac{4}{8} \tanh \end{aligned}$$

Owing to the modified Matsubara frequencies, these sums are computed with a modified Fermi distribution, $f(\omega) = (\text{e}^{\omega} + 1)^{-1}$. Defining the dimensionless control parameter $\epsilon = \frac{2}{k}$, the effective action is transformed back to imaginary time at zero temperature.

$$S_{\text{eff}} = \int_0^{\infty} d\omega \left[\frac{1}{2} (m + \frac{2}{4}) \underline{x}^2 + \frac{1}{2} k (1 - \underline{x}^2) + \frac{4}{8} \underline{x}^4 \right]$$

The mass is enhanced by a dynamical quantity and, most significantly, the action exhibits an instability at $\epsilon = 1$. When $\epsilon > 1$ and $\omega = 0$, the action is minimized for $x_0 = -(\frac{2}{2})^{1/2}$. For $\epsilon \neq 0$, there is no true broken symmetry, however an approximate calculation of the instanton action

$$S_i = \frac{p}{2} \frac{(-1)^{3/2}}{\frac{1}{2}} \frac{r}{1 + \frac{1}{2}} \quad (3)$$

reveals that, although the symmetry changes at $\epsilon > 1$, the instanton is only stabilized for $\epsilon > 1$. This defines the entangled regime of the qubit and oscillator.

Now we must find the corresponding dynamics of the qubit, in particular, the spin-spin correlation function. It may be shown that

$$hT_{ij}(\omega) = \frac{1}{Z} \int_0^{\infty} D\omega_n D\omega_m hT_{ij}(\omega) i S_f[x] e^{S_{\text{eff}}}$$

where $S_f[x]$ denotes averaging over the fermionic action for a particular realization of the boson field $x(\omega)$. By Wick contractions, this average is related to the single fermion Green's function, in the presence of an inhomogeneous field $x(\omega)$, which solves the equation of motion: $(\partial + \omega_x + x(\omega)_z) G(\omega; x(\omega)) = \delta(\omega)$. This approach has been used to implement bosonization in 1-d fermion systems.⁸ In the present case, the Green's functions must satisfy the boundary conditions implied by the shifted Matsubara frequencies: $G(\omega = 0) = iG(\omega_0)$. Furthermore, the boson field x must be written as the sum of an instanton trajectory and a small oscillation: $x(\omega) = x_i(\omega) + r(\omega)$. We now make the non-Abelian Schwinger ansatz,⁹

$$G(\omega; x(\omega)) = U(\omega) g(\omega; x_i(\omega)) U^{-1}(\omega); \quad (4)$$

where g satisfies the equation of motion but with the field $x(\omega)$ restricted to the instanton trajectory: $(\partial + \omega_x + x_i(\omega)_z) g(\omega; x_i(\omega)) = \delta(\omega)$, and $x_i(\omega) = x_0$. Now $U(\omega)$ must satisfy the auxiliary condition

$$[\partial U + H^*; U] = -r(\omega)_z U \quad (5)$$

where $H^* = \omega_x + x_i(\omega)_z$.

A solution of the equation of motion for g which satisfies the boundary conditions is obtained for all ω away from the instanton kinks (consistent with the dilute gas approximation); for $\omega < \omega_0$

$$\begin{aligned} g(\omega; x_i(\omega)) &= \frac{1}{2} f(\omega) \left[1 + \frac{1}{\omega_x} \right] + \frac{x_i(\omega)}{\omega_z} e^{-\omega_x(\omega - \omega_0)} \\ &+ \frac{1}{2} f(\omega) \left[1 - \frac{1}{\omega_x} \right] + \frac{x_i(\omega)}{\omega_z} e^{-\omega_x(\omega - \omega_0)} \end{aligned}$$

where ω is the Rabi energy $\omega = \frac{p}{\omega_x^2 + \omega_z^2}$. The Green's function $g(\omega > \omega_0)$ is obtained by the replacement $f(z) \rightarrow f(z)$ where $f(z) = f(-z)$. The auxiliary condition (5) leads to a set of Riccati equations for an appropriate parameterization of U which are difficult to solve generally.⁹ In the strong coupling limit (i.e. to lowest order in ϵ) the interacting Green's function is found to be $G(\omega; x(\omega)) = g(\omega; x_i(\omega)) \exp(-\omega_z r(\omega) d)$.

Within this scheme we need to evaluate $c_{zz}(\omega)$ = $hT_{zz}(\omega) z(\omega) i S_f[x]$; other correlation functions are obtained similarly. $c_{zz}(\omega)$ involves two contractions yielding a DC part of c_{zz} and a part at energy 2ω , respectively. These correlation functions must in turn be

averaged over the effective boson action, S_e .

$$\begin{aligned} hT \int dz (\partial_z \phi^0) i &= h \lim_{1!} \text{tr}_z G(1; x(1)) \\ &\quad + \lim_{2!} \text{tr}_z G(2; x(2)) i_{\text{eff}} \quad (6) \\ &\quad + h \text{tr}_z G(0; x(0)) \int dz G(0; x(0)) i_{\text{eff}} \end{aligned}$$

The first contraction in (6) will involve products of $x_i(\cdot)$ at different times, giving the proper long time behavior; the second contraction will involve the average over boson fluctuations $r(\cdot)$ that dress the qubit oscillations at energy γ . To evaluate the average over S_e we need both boson correlation function. Within the instanton approximation, the first contraction in (6) involves

$$hT \int dz (\partial_z \phi^0) i_{\text{eff}} = x_0^2 e^{-j\gamma} \quad (7)$$

where $\gamma = \frac{1}{2} \sum_{i=2}^p \exp S_i$. The second contraction in (6) involves the average over fluctuations of $r(\cdot)$, $h \text{tr}_z d r(\cdot) i_{\text{eff}}$. Averages of this form and their Fourier transforms have been discussed in several places¹⁰. The relationship to the FGM¹¹ may now be seen: Replacing (in ref.⁹) the 1-d spatial degree of freedom in the FGM by imaginary time, eqn. (2) is the action for a fermion of frequency i propagating in a Peierls chain with a gap function $x(\cdot)$. Averaging (in eqn. (6)) over the instanton fluctuations of $x(\cdot)$ with correlator (7) is equivalent to the disorder average in ref.⁹ with a correlation length given by the instanton time,

¹. In the FGM, the density of states at the Fermi surface is accessed by the zero frequency limit $\lim_{1!} i 0^+$ which corresponds to $\lim_{1!} 0^+$, the strong coupling limit in the present work. The two models differ in that the correlation length of the gap disorder in the FGM is an independently controlled parameter whereas the instanton fluctuations are generated spontaneously in the present model. In addition, the fermions in the present model satisfy twisted boundary conditions.

Continuing to real frequencies and denoting the imaginary part of the Fourier transform of (6) by $s_{zz}(\omega)$, we obtain for $\omega > 1$ a correlation function of the form

$$\begin{aligned} s_{zz}(\omega) &= \frac{1}{2} \left(\frac{x_0}{\omega} \right)^2 (1) \\ &\quad + \frac{1}{2} \left(1 - \left(\frac{x_0}{\omega} \right)^2 + \left(\frac{1}{\omega} \right)^2 \right) \\ &\quad \times \frac{p^{n+m} e^{2p}}{m \ln n} (1 - 2^{\omega} (n-m)!) \quad (8) \end{aligned}$$

for $\omega > 0$ where $p = \frac{1}{2}$. This is our main result. Equation (8) shows that for the broken symmetry phase ($\omega > 1$) two distinct spectral features are formed. The low energy feature with weight $w_{\text{ent}} = \frac{1}{2} \left(\frac{x_0}{\omega} \right)^2$ ($\omega < 1$) corresponds to the qubit entangled with the oscillator and in a superposition of the form $|j; + x_0 i \rangle$; $x_0 i$, where $j+$ refer to states of the qubit with nonvanishing z -polarization. The high energy set of delta functions (at energy $\omega = 2\gamma$), corresponds

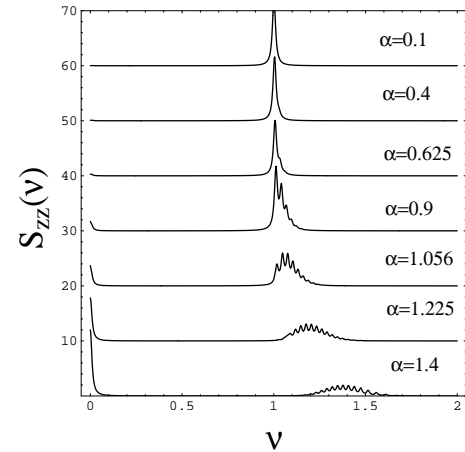


FIG. 1: Numerical diagonalization of Hamiltonian (1). Dynamical spin-spin correlation function showing the emergence of the low energy instanton feature corresponding to entanglement. In this calculation, $! = 0.01$; $= 0.5$; $k = 0.4$. Peaks are artificially broadened and vertical scale on curves for the largest four values of α magnified 2.

to the decoupled (unentangled) but dephased qubit with weight $w_{\text{free}} = 1 - \frac{1}{2}$. Although the spectrum is discrete, dephasing may be estimated by considering the envelope of the sidebands associated with the primary resonance. For small α (large p) the Poisson distributions become approximately Gaussian and the dephasing rate is estimated to be $\propto p^{1/2}$; the fractional width of the resonance, $1-Q$, is then $\propto \frac{1}{p} p^{1/2}$. The qubit becomes critically damped when this factor is unity. When $\alpha = 1$, keeping k and therefore γ constant, the width of the resonance goes to zero as $O(m^{-1/4})$ (although the number of bosons diverges), in agreement with the classical calculation.

The spectral weights appearing in equation (8) satisfy the sum rule: $w_{\text{ent}} + w_{\text{free}} = 1$. At critical coupling, a redistribution of spectral weight is initiated and spectral weight flows from the coherent feature to the entangled one. Unlike the SBM where the system spin becomes overdamped before it becomes localized, coherent and effectively localized behavior coexist in the present model¹². An approximate numerical diagonalization of the Hamiltonian (1) confirms these results. The Hilbert space of H was truncated to 100 states; no systematic changes were observed in increasing the cut-off of the Hilbert space. Figure 1 shows the correlation function $s_{zz}(\omega)$ through the transition to the entangled regime. A low energy feature is seen that agrees closely with the parameters of this calculation and the calculated instanton frequency γ . The primary resonance is broadened by oscillator fluctuations but not overdamped and thus remains distinct from the instanton feature. As expected, $w_{\text{ent}}^{1/2}$ is the order parameter for a second order phase transition. The emergence of low frequency spectral weight for $\omega < 1$ in figure 1 is a consequence of $n! = 1$, not an artefact of the truncation of the Hilbert space;

in the strict adiabatic limit ($\omega_0 \ll \omega$), the derivative $\frac{d\omega}{d\omega_0} = 2$ would diverge.

One practical consequence of our results is that when the environment responsible for dephasing the qubit is strongly monochromatic, the resonant contribution to dephasing described here may become the dominant source of decoherence over the weak-coupling contribution from the bath continuum. As an example, we now turn to experimental realizations of superconducting qubits. Several recent designs for superconducting qubits involve persistent current SQUIDS and/or Cooper boxes apparently coupled to a measurement DC-SQUID. The state of the qubit is ultimately read by ramping the current through the measurement DC-SQUID until it switches from the superconducting to voltage branch. The qubit system that we study consists of a persistent current qubit inductively coupled to a measurement DC-SQUID. In¹ it was demonstrated that the dominant source of decoherence in the qubit was the Nyquist voltage fluctuations in the electromagnetic environment of the DC-SQUID. This environment may be characterized¹³ by a single impedance $Z(\omega)$ including the SQUID itself (an inductance L_J) in parallel with the junction and shunt combined capacitance, C , and a resistance, R . De-phasing results follow from the spin-boson model where $J(\omega) = \frac{1}{i} R e Z(\omega) = R e \left(\frac{1}{R} + i \omega C + \frac{1}{i \omega L_J} \right)^{-1}$; in particular, J is ohmic at low frequencies.

However, the spectrum $J(\omega)$ is highly structured, dominated by the plasma mode at the frequency $\omega_0 = 1/\sqrt{L_J C}$ with a $Q = 10$ for typical parameters¹. To compute the resonant contribution to decoherence, the parameters of the action (2) must be found in terms of the DC-SQUID parameters. The inductive coupling to the qubit comes from the circulating component of current in the DC-SQUID. Denoting the DC-SQUID phase variable combinations $\frac{1}{2}(a + b)$, $\frac{1}{2}(a - b)$ by ϕ , respectively, the circulating current is given by: $I_c = 2I_0 \sin \frac{1}{2} \phi$, where I_0 is the critical current of both junctions and ϕ is the dimensionless flux in the DC-SQUID, $\phi = \frac{2\pi}{\Phi_0}$. The effective potential of the DC-SQUID is then $U(\phi) = -2I_0 \cos \frac{1}{2} \phi$, where I_0 is the external current flowing through the

DC-SQUID. Choosing an "operating point" for the DC-SQUID, $\phi = 2$ and $q = 1$, determined by minimizing $U(\phi)$, we find $k = \frac{1}{2} \sqrt{4I_0^2 \cos^2 \frac{1}{2} \phi - I_0^2}$. Thus the effective potential softens and the dimensionless coupling constant $\kappa = \frac{1}{k}$ increases as I_0 approaches the switching value. Linearizing the circulating current about the operating point we obtain $I_c = 2I_0 \sin \frac{1}{2} \phi \sin \frac{1}{2} \phi$. The effective coupling constant, neglecting the mutual inductance (M) between the persistent current in the qubit (I_p) and circulating current of the DC-SQUID is then $\kappa = 2M I_0 I_p \sin \frac{1}{2} \phi \sin \frac{1}{2} \phi$. Finally, the mass appearing in action (2) is proportional to the capacitance of the junctions: $m = C_0 = (2\pi)^2$.

To illustrate our point, we use $M = 20 \text{ pH}$, $I_p = 900 \text{ nA}$ and $I_0 = 150 \text{ nA}$ and estimating that the SQUID switches when I_0 reaches 0.95 of the critical switching value, $2I_0 \cos \frac{1}{2} \phi$, and obtain a dimensionless coupling of

1. The resonant contribution to dephasing becomes significant when $\omega = \omega_0 > 1$ in which case $Q = (\omega/\omega_0)^{1/2}$. Using $\omega_0 = 1$ and the adiabatic ratio $\omega_0/\omega = 10$, yields a $Q = 3.3$. As in fig. 1, the spectrum is of course discrete, consisting of several sidebands. The ohmic spectrum, $J(\omega) = \omega$, for the same DC-SQUID parameters has a dimensionless coupling of $\kappa = 0.03$ corresponding to coherent behavior of the qubit with very weak damping (see refs.^{1,14} for details.)

In conclusion, we have considered a model in which a qubit is strongly coupled to a single environmental mode and described the resulting dephasing and entanglement. In contrast to weak-coupling approaches, qubit backaction on the environment is shown to play a central role, leading to a symmetry change in the bosonic effective potential and the appearance of coexisting localized and coherent behavior for the qubit. Although these are general results, this model may apply to underdamped quantum detectors of a qubit. Finally, we have shown that the spin-oscillator model has an unexpected correspondence with a Hamiltonian for disordered fermions in the Fluctuating Gap Model.

We thank Jeremy Layfield, Boris Fine, Philip Stamp, and Oleg Starykh for many useful discussions.

¹ C. H. van der Wal, et al., *Science* 290, 773 (2000); C. H. van der Wal, Ph.D. dissertation, Delft (2001).

² D. Vion, et al., *Science* 296, 886 (2002).

³ Y. M. Aikhlin, G. Schon, and A. Shnirman, *Rev. Mod. Phys.* 73, 357 (2001).

⁴ D. V. Averin, preprint cond-mat/0004364.

⁵ A. A. Clerk, S. M. Girvin, and A. D. Stone, preprint cond-mat/0211001.

⁶ D. M. Ozyrsky and I. Martin, *Phys. Rev. Lett.* 89, 018301 (2002).

⁷ V. N. Popov and S. A. Fedotov, *Sov. Phys. JETP* 67, 535 (1988).

⁸ D. K. K. Lee and Y. Chen, *J. Phys. A: Math. Gen.* 21,

4155 (1988).

⁹ L. Bartosch and P. Kopietz, *Phys. Rev. Lett.* 82, 988 (1999).

¹⁰ See, for instance, G. M. Khan, *Many-Body Physics*, Plenum Press, 1981 (Sec. 4.3).

¹¹ P. A. Lee, T. M. Rice, and P. W. Anderson, *Phys. Rev. Lett.* 31, 462 (1973).

¹² G. Levine and V. N. Muthukumar, *Phys. Rev. B* 63, 2451 (2001).

¹³ A. J. Leggett, *Les Houches, Session XLV I*, (1986).

¹⁴ L. Tian, S. Lloyd, and T. P. Orlando, *Phys. Rev. B* 65, 144516 (2002).